
2-3-6 Ionosphere Simulation

SHINAGAWA Hiroyuki

Space weather forecasts are about to enter a stage incorporating numerical forecasts based on full-scale numerical simulation, in addition to conventional methods used by forecasters to make predictions based on observational data and experience. NICT is currently running a real-time integrated simulator for space weather developed under the leadership of the Space Environment Group. This system consists of three real-time simulators used for the sun and solar wind, the magnetosphere, and ionosphere, respectively. In the system, the simulation data is made available to the public immediately. This paper gives an overview of the ionospheric model used in this system and presents an example of real-time ionospheric simulation results.

Keywords

Space weather, Ionosphere, Numerical forecast, Simulation, Magnetic storm, Real time

1 Introduction

The atmospheric region at an altitude of more than 80 km is called the upper atmosphere and is a mixture of neutral gas and ionized gas consisting of ions and electrons. The thermosphere is an extremely thin atmospheric region with density less than 1/100,000 of the atmosphere at the ground surface. The ionosphere has even lower density by several digits and is so thin that it can almost be called a vacuum. However, it is an important region for human activity. For example, communications and radio broadcasts using short waves are conducted through reflection in the ionosphere. If the ionosphere becomes unusually ionized through X-rays resulting from a solar flare or falling energetic particles from magnetic storms, it will disrupt communications and broadcasts, perhaps even affecting our lives. Moreover, when a severe magnetic storm occurs, significant energy flowing into the ionospheric region in the form of auroral particles causes strong heating and expansion of the thermosphere, resulting in a dramatic increase of the atmospheric density. In such an event, a low-altitude earth orbiter at about 400

km or lower will experience difficulty in controlling its orbit because of exposure to strong atmospheric drag, and may even fall into the earth in the worst-case scenario. By understanding the current conditions of the upper atmosphere and predicting the future state, appropriate measures could then be taken to prevent or alleviate damage. At the moment, certain research institutes in the world are developing numerical prediction models for various ionospheric disturbances.

2 Ionospheric simulation

2.1 Development of the ionospheric models

Theoretical studies on the ionosphere began in the 1960s. With the development of computers, realistic simulation models were first built around 1970. The first model—the vertical one-dimensional diffusion model—was developed by Schunk et al. at Utah State University, who successfully reproduced the basic structure and daily changes of the mid-latitude ionosphere for the first time [1]. Later in the 1980s, global three-dimensional models were developed by several groups in the

USA [2]. This made it possible to examine theoretically how polar region disturbances associated with magnetic storms affect the global ionospheric environment [3]–[5].

The ionosphere is characterized by the fact that it is heavily affected by the magnetospheric electric field, high-energy particles (auroral particles) and waves propagating from the upper and lower atmospheres. In the first model, the effects of the thermosphere and magnetosphere were given from an empirical model. The 1990s witnessed the development of both a magnetospheric model and a thermospheric model. The first magnetosphere-ionosphere-thermosphere coupled model was developed around 2000 [6]. In the present century, the models in each region were further improved in terms of precision, while efforts were initiated to develop a model of solar surfaces and solar winds, and a “solar-terrestrial environmental integrated model” that includes all regions from the lower atmosphere to the thermosphere [7].

However, numerical models based on the fluid equations cannot, in principle, represent the effects of microscopic phenomena such as turbulent flows and the particle-level effects such as auroral particles. For that reason, empirical input data, empirical equations, and other parameters were introduced into the model with their effects being taken in. Such a technique (called parameterization) is commonly used in many global models. To increase the precision of numerical models, it is essential to compare observational data and models, and enhance the technique of parameterization.

2.2 Method of ionospheric modeling

Many ionospheric models have been developed by research institutes in various parts of the world, along with various types of equation systems and methods of modeling, ranging from very simple ones to those highly rigorous. Here, the most widely used and relatively simple method is presented. The NICT model is also based on the method presented below.

The ionosphere can be represented by a fluid equation consisting of ions and electrons. The general equation system used in ionospheric models is shown below.

Continuity equation

$$\frac{\partial n_i}{\partial t} = -\nabla \cdot (n_i \mathbf{v}_i) + P_i - L_i \quad \dots\dots\dots (1)$$

Ion momentum equation

$$\frac{\partial \mathbf{v}_i}{\partial t} = -(\mathbf{v}_i \cdot \nabla) \mathbf{v}_i - \frac{1}{m_i n_i} \nabla p_i - \nu_{in} (\mathbf{v}_i - \mathbf{v}_n) + \mathbf{g} + \frac{e}{m_i} (\mathbf{E} + \mathbf{v}_i \times \mathbf{B}) \quad \dots\dots\dots (2)$$

Electron momentum equation

$$\frac{\partial \mathbf{v}_e}{\partial t} = -(\mathbf{v}_e \cdot \nabla) \mathbf{v}_e - \frac{1}{m_e n_e} \nabla p_e - \nu_{en} (\mathbf{v}_e - \mathbf{v}_n) + \mathbf{g} - \frac{e}{m_e} (\mathbf{E} + \mathbf{v}_e \times \mathbf{B}) \quad \dots\dots\dots (3)$$

Ion energy equation

$$\frac{3}{2} n_i k \frac{\partial T_i}{\partial t} = -\nabla \cdot \mathbf{q}_i - \sum_i \frac{n_i m_i \nu_{it}}{m_i + m_t} \left[3k(T_i - T_t) + m_t (\mathbf{v}_i - \mathbf{v}_t)^2 \right] \quad \dots\dots\dots (4)$$

Electron energy equation

$$\frac{3}{2} n_e k \frac{\partial T_e}{\partial t} = -\nabla \cdot \mathbf{q}_e + Q_e \quad \dots\dots\dots (5)$$

where, n denotes density, \mathbf{v} velocity, P rate of particles generated, L loss rate of particles, m mass, ν_{ab} momentum transfer collision frequency of “ a ” particles with regard to “ b ” particles, p pressure, \mathbf{g} gravity acceleration, q heat flow velocity, and Q net heating rate. Suffixes i , n and e denote i -type ions, n -type neutral particles, and electrons, respectively, and suffix t also represents all particles.

In the continuity equation (1), the production of ions involves photoionization where the solar extreme ultraviolet radiation (EUV) directly ionizes neutral particles, together with the contribution of secondary ionization where ionization-induced electrons (photoelectrons) ionize the surrounding neutral atmosphere. Since a rigorous calculation of ionization induced by photoelectrons is rather complex, a simple equation of approximation is common-

ly used. Moreover, there are many chemical reactions between ions and neutral particles, so that a certain ion produces another kind of ion also included in the generation. Ions disappear through an ion chemical reaction, but dissociative recombination eventually combines ions with electrons, thereby turning them back into neutral particles and disappearing. The photochemical process is predominant below 200 km in altitude, while in the F layer of the ionosphere above 200 km, the term of transportation in the first term on the right side in equation (1) is important. In that region, the diffusion process of ions and the effects of convection by the electrical field are predominant.

In the ion momentum equation (2), temporal changes in the first term on the left side and the inertia term in the first term on the right side are relatively small and therefore ignored at times, but such changes are not necessarily small in the upper ionosphere. Moreover, in strict terms, a viscosity term for ions may be added. In the electron energy equation (3), temporal changes and the term of inertia can normally be ignored.

In the equations for ion and electron energy (4) and (5), local temporal changes in the first term on the left side are small and may be ignored; these changes can be expressed in the form of balance between the term of heating and cooling, and the term of thermal conduction. As an uncertain factor, there is a heat flux given as an upper boundary condition. Neglecting to add this condition is known to result in unrealistic ion or electron temperatures, so that an appropriate value is given to match the observations.

In ionospheric simulations, the basic procedure involves solving these equations, but in the case of the earth's ionosphere, the intrinsic magnetic field is sufficiently strong at ionospheric altitudes, and one can safely assume that the form of magnetic lines remains unchanged. In solving the momentum equations, therefore, the method described below is used in many cases for the sake of convenience.

First, ignore the term of temporal changes in the momentum equation and divide the velocity into the component parallel to the magnetic lines (suffix //) and the vertical component (suffix \perp).

$$\mathbf{v}_i = \mathbf{v}_{i//} + \mathbf{v}_{i\perp} \quad \dots\dots\dots (6)$$

The motion of ions perpendicular to the magnetic lines can be expressed as follows:

$$\mathbf{v}_{i\perp} = \mathbf{v}_n + \frac{e}{v_{in}m_i}(\mathbf{E}_{\perp} + \mathbf{v}_{i\perp} \times \mathbf{B}) \quad \dots\dots\dots (7)$$

This can be solved with regard to $\mathbf{v}_{i\perp}$ to determine the velocity.

On the other hand, the motion parallel to the magnetic lines can be expressed with regard to electrons and ions as follows:

$$0 = -\frac{1}{n_e m_e} \nabla p_{e//} - v_{en}(\mathbf{v}_{e//} - \mathbf{v}_{n//}) + \mathbf{g}_{//} - \frac{e}{m_e} \mathbf{E}_{//} \dots (8)$$

$$0 = -\frac{1}{m_i n_i} \nabla p_{i//} - v_{in}(\mathbf{v}_{i//} - \mathbf{v}_{n//}) + \mathbf{g}_{//} + \frac{e}{m_i} \mathbf{E}_{//} \dots (9)$$

Delete $\mathbf{E}_{//}$ from that and one will obtain the velocity. Now, think of a simple case and assume that ion i is the main ion. Using the approximations $n_i = n_c$, $v_{in} \gg v_{en}$, and $m_i \gg m_e$, one can obtain the result as follows:

$$\mathbf{v}_{i//} = -\frac{e}{m_i n_i v_{in}} (\nabla p_i + \nabla p_e) + \frac{\mathbf{g}_{//}}{v_{in}} + \mathbf{v}_{n//} \quad \dots\dots (10)$$

The motion parallel to the magnetic lines can be expressed in the form of a diffusion equation in a magnetic field flux tube, and the direction perpendicular to the magnetic lines is expressed as motion $\mathbf{E} \times \mathbf{B}$ to which an electrical field is added. In that case, \mathbf{E} becomes the convection electrical field of the magnetosphere at high altitudes and the dynamo electrical field at mid-to-low altitudes.

3 Real-time simulation model of the ionosphere at NICT

3.1 Real-time ionospheric simulation

NICT has developed an ionospheric model on its own and is now conducting ionospheric simulations on a real-time basis. This model is

designed to solve the three-dimensional basic equations of the ionosphere mentioned above in real time, in order to determine ionospheric quantities. Background neutral atmospheric structure is given by an empirical model. The ionospheric model includes a thermospheric model, which is designed to determine perturbation quantities of the neutral atmosphere, and can express thermospheric changes. In addition, the effects of the magnetosphere are included by using the electric conductivity and potential of the polar regions as obtained from the real-time magnetospheric model operating at the same time. The real-time magnetospheric model uses real-time solar wind data obtained from the ACE solar observation satellite.

As such, real-time solar wind data is used as input, so that the system can reproduce the present conditions of the ionosphere and thermosphere. This system has been in operation since July 2008, and information obtained by the system is available to the public on the Web. The following describes an overview of this ionospheric model.

3.2 Ionospheric model

The coordinate system employs a spherical coordinate system (vertical, latitude, longitude) for both the thermosphere and the ionosphere. The vertical extent of the neutral atmosphere ranges from 0 km (ground surface) to 600 km with the 10-km grid interval. The ionospheric model ranges from 0 km (ground surface) to 3000 km, including the 10-km grid interval up to an altitude of 600 km, and above that, the interval gradually increases until becoming 100 km near the upper boundary. The grid points in the directions of latitude and longitude are set at intervals of 1 and 5 degrees, respectively. A spherical coordinate system used on global simulations is generally disadvantageous in that the interval between grid points close to the poles narrows rapidly, but it is not necessarily a disadvantage in ionospheric simulation because upper atmospheric phenomena are often accompanied by small-scale phenomena such

as auroras at high altitudes. However, the grid points narrow down more than necessary near the poles, so that regions within 3 degrees from the poles are deprived of grid points and the values are calculated by interpolation.

The ionosphere involves five types of ions (N_2^+ , O_2^+ , NO^+ , O^+ , H^+). The method described is used regarding the equation of motion, and the density ratio of O^+ and H^+ is empirically given and regarded as a one-fluid ion divided into two velocity components (diffused in the magnetic line direction and drifted by $\mathbf{E} \times \mathbf{B}$ in the direction perpendicular to the magnetic line), and the velocity is determined based on equations (7) and (10). Moreover, photochemical equilibrium is assumed to determine the density of molecular ions.

Regarding the equation of energy, the ions are designed not to be within the term of temporal changes on the left side of equation (3) with thermal conductivity excluded. For electrons as well, the term of temporal changes on the left side of equation (5) are ignored and, in the lower ionosphere (at about 150 km or lower), an exchange of energy occurs through collisions and photoelectron-induced heating. In the upper ionosphere (at about 250 km or higher), thermal conduction alone is set to be effective and given by an analytical solution, and the solutions for the upper and lower ionospheres are smoothly connected. The shape of the magnetic field is approximated with the dipole field. Moreover, a dynamo electric field generated by the neutral wind is included using a separately built dynamo model [8].

Model input utilizes a solar EUV spectral model EUVAC [9] based on F10.7 using solar radio intensity as a proxy. The ionization rate, heating rate, and electric potential in the polar regions are given by an empirical formula based on the output data of the magnetospheric model.

3.3 Thermospheric model

The ionospheric simulator incorporates a neutral atmospheric model using an empirical model as a basic state. This part of the model

can be replaced with another atmospheric model. This model is characterized by the fact that, in order to solve small-scale phenomena temporally and spatially with high precision, the compressible fluid equation system for a nonhydrostatic equilibrium is used instead of a model of hydrostatic approximation, which is used in many global atmospheric models.

The general equation system used in neutral atmospheric models is shown below.

Continuity equation

$$\frac{\partial \rho}{\partial t} = -\nabla \cdot (\rho \mathbf{v}_n) \quad \dots\dots\dots (11)$$

Neutral momentum equation

$$\begin{aligned} \frac{\partial \mathbf{v}_n}{\partial t} = & -(\mathbf{v}_n \cdot \nabla) \mathbf{v}_n - \frac{1}{\rho} \nabla p + \mathbf{g} - 2\boldsymbol{\Omega} \times \mathbf{v}_n \\ & - \nu_{ni} (\mathbf{v}_n - \mathbf{v}_i) + \frac{1}{\rho} \nabla (\mu \nabla \cdot \mathbf{v}_n) \quad \dots\dots (12) \end{aligned}$$

Neutral energy equation

$$\begin{aligned} \frac{\partial T}{\partial t} = & -(\mathbf{v}_n \cdot \nabla) T - \frac{R}{C_v} T (\nabla \cdot \mathbf{v}_n) \\ & + \frac{1}{\rho C_v} \frac{\partial}{\partial z} \left(\kappa \frac{\partial T}{\partial z} \right) + \frac{Q}{C_v} \quad \dots\dots\dots (13) \end{aligned}$$

Equation of state

$$p = \rho R T \quad \dots\dots\dots (14)$$

where, ρ denotes mass density, \mathbf{v}_n velocity, p pressure, R gas constant, T temperature, C_v specific heat at constant volume, μ molecular velocity, κ thermal conductivity coefficient, Q net heating rate, and $\boldsymbol{\Omega}$ angular velocity of rotation.

The atmosphere is designed as single fluid with its composition consisting of three elements: O, N₂, and O₂. For the basic field, the atmospheric density and temperature are given by empirical model NRL-MSISE00 [10], while the ratio of composition is calculated based on the composition ratio of the basic field [11]. The basic field for velocity is designed as given by empirical model HWM93 [12]. In actual calculations, this basic field is assumed to be in a steady-state equilibrium, and the amount of change (such as $\rho' = \rho - \rho_0$) from

that state is solved. The method of numerical solution is the finite difference method, while the advection terms are solved using the CIP method.

3.4 Coupling to the magnetosphere

The response of the ionosphere to magnetospheric inputs and feedback processes from ionospheric variations to the magnetosphere (i.e., the process of interaction between the magnetosphere and ionosphere) remain unsolved and are a major challenge. Numerical simulation is an effective means of addressing this issue. However, in terms of model connection, the issue is to find an effective way to exchange mutual information. Of particular importance is how to give electric conductivities of the polar ionosphere corresponding to ionization caused by auroral particles falling from the magnetosphere. Our magnetospheric model is based on a spherical shell-shaped ionosphere and projects the parameters of the magnetosphere's inner boundaries ($r = 3.5 R_e$) onto the ionosphere. The electric conductivity of the ionosphere is given as a height-integrated value, and is supposed to be determined by three components: (1) an electric conductivity component corresponding to solar extreme ultraviolet radiation (EUV), (2) a component corresponding to diffuse aurora (and set to a function of plasma pressure and mass density on the plasma sheet in the magnetospheric model), and (3) a component corresponding to discrete aurora (and set to a function of field-aligned currents in the polar regions of the magnetospheric model). This function is empirically given to reproduce observations as effectively as possible.

Using the height-integrated electric conductivity, altitude distribution of the electric conductivity is determined and used as three-dimensional data in the ionospheric model. This electric conductivity is then used to estimate the ion production rate, the plasma heating rate, and the neutral particle heating rate. This series of procedures is called parameterization—a method necessary for entering

microscopic effects into a global model.

The electric potential of the polar regions is another important parameter for the ionosphere. Since it is directly given by the magnetospheric model, this parameter is used as input for the polar electric field of the ionospheric model. For ionized components associated with EUV on the dayside, input parameters are calculated in the ionospheric model. With this method, using the solar wind as an input enables the execution of a model that reproduces ionospheric and thermospheric conditions on a real-time basis.

3.5 Example of real-time simulation results

Here we introduce an example of calculations obtained from the real-time model. Figure 1 shows the actual results obtained from a real-time simulation on July 23, 2008. It shows the electron density and plasma velocity at an altitude of 120 km. With a rise in the southward component of the solar wind magnetic field, disturbances occurring in the magnetosphere result in disturbances in the ionosphere as well. The night side (bottom) of the figure shows a crescent-shaped region with high electron density; this is an “aurora” reproduced on a computer. The bright region

at the top is due to the effects of ionization stemming from solar ultraviolet radiation on the dayside. Given the insufficient resolution of the model, the aurora microstructure cannot be reproduced, but its overall structure agrees well with the representative observation results shown in Fig. 2. The convection velocity of ionospheric plasma excited in the electric field of the magnetosphere exceeds 1 km/s, thereby indicating the occurrence of fast convection.

Figure 3 shows increases in temperature and wind speed in the thermosphere at an altitude of 300 km at the same time of day as in Fig. 1. Both figures show the amount of deviations from the atmosphere in a steady state. When a magnetic storm occurs over the polar regions, the energy of the solar wind flows into the upper atmosphere, and dramatically increases thermospheric and ionospheric temperatures. This heating enhances the thermospheric pressure in the polar regions, thereby driving strong winds from the poles to flow toward the equator. These winds elevate the ionosphere, resulting in increased electron density at mid-latitudes. Such a disturbance

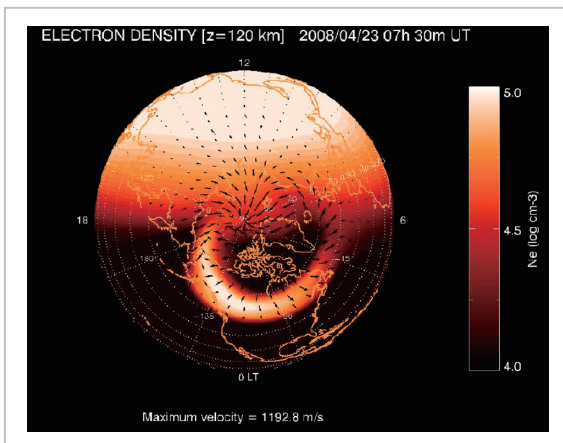


Fig. 1 Electron density distribution and plasma velocity at an altitude of 120 km as obtained in real-time ionospheric simulation

The crescent-shaped bright region on the nighttime side (bottom) represents the aurora in the simulation.

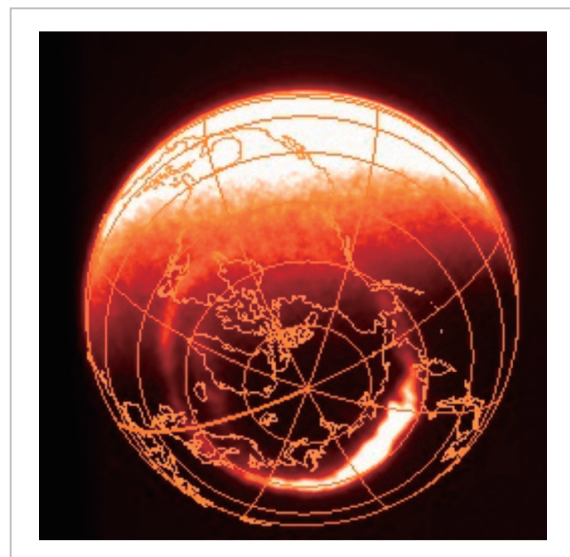


Fig. 2 Auroral image taken in outer space from an artificial satellite (courtesy: Space Sciences Laboratory, University of California, Berkeley)

This is an image taken on a day other than when the image in Fig. 1 was taken, but does show the characteristic aurora structure.

involving increased electron density is called a positive storm.

As the thermospheric atmosphere becomes heated, it also expands, thereby increasing the neutral atmospheric density in high-altitude

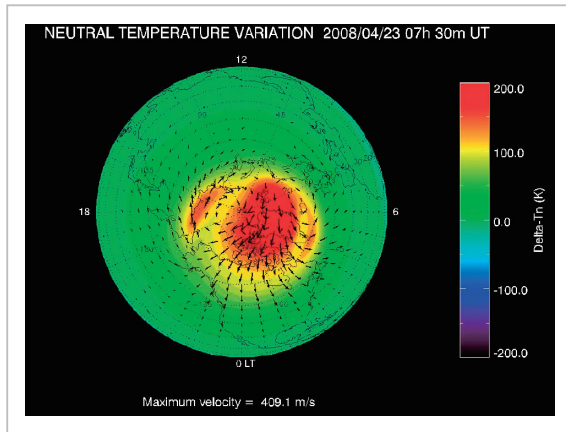


Fig.3 Increases in temperature (color contours) and wind velocity (arrow) in the thermosphere at an altitude of 300 km in the Northern Hemisphere

Both represent the amount of changes from the atmosphere in a steady state. The red regions represent the heated portions, along with rising atmospheric density. Thermospheric winds flow toward the equator from these heated regions. The center represents the North Pole; the top represents the daytime side.

regions. In the event of extreme disturbances, atmospheric drag will alter artificial satellite orbits, and in the worst cases cause a satellite to fall from orbit. Such drag may even change the distribution of space debris, which is now regarded as a serious problem. Expansion of the thermospheric atmosphere is an extremely important phenomenon in terms of space weather as well as in other respects.

Figure 4 shows an example of positive storms actually reproduced in the ionosphere through real-time ionospheric simulation. This disturbance occurred on June 25, 2008. This event is an example of heating that occurs in the polar regions, resulting in thermospheric winds directed toward the equator, and causing an increase in the total electron content (TEC) of the ionosphere. The disturbance is relatively small in scale, but when compared with the trend of changes in TEC over Kokubunji as observed with GPS satellites, the model reproduces a trend where its TEC increased around the end of the 14th and became higher than the average on the 15th, thus showing that the simulation agrees well with the observations.

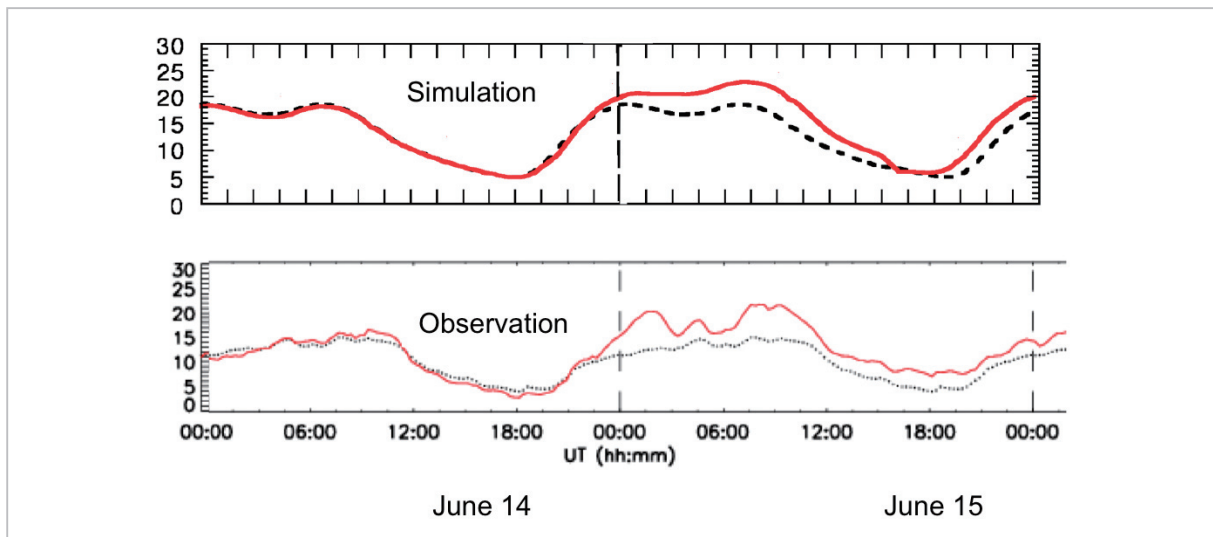


Fig.4 Changes in the total electron content (in $10^{16}m^{-2}$) in the ionosphere on days of ionospheric disturbance (June 14 and 15, 2008) (red line) near Tokyo

(Top) Calculation results of the real-time space weather simulator (bottom) total electron content of the ionosphere obtained in observation. The dotted line represents the variation during quiet days in the ionosphere. The model reproduces the enhancement in electron density compared with that on quiet days from the end of June 14 to June 15.

4 Conclusion

This paper gave an overview of the ionospheric model and related techniques. At present, continual operation is conducted on the real-time space weather integrated simulator of NICT, while comparing ionospheric changes with various observational data on the ionosphere, and thereby validating the magnetosphere-ionosphere coupling. Although this simulation needs to be further improved in quantitative terms, ionospheric changes in the simulation agree fairly well with observations regarding many disturbances stemming from the magnetosphere. This leads us to consider the possibility of developing a numerical prediction model for the ionosphere covering a period of about several hours. Moreover, ionospheric disturbances stemming from the lower atmosphere are also important at mid to low latitudes. To adopt such disturbances, it is necessary to use an extended atmospheric model including meteorological phenomena as

well. To that end, efforts are now under way to develop a model [13] and compare it with observational data [14][15].

Coping sufficiently with space environment disturbances in practical applications often requires predictions half a day to about several days in advance. To that end, it is indispensable to perform numerical predictions not only on the magnetosphere and ionosphere but also on the solar wind on the upstream side. Since 2008 we have been operating a real-time simulator for the sun and the solar wind as well. The data obtained is now being compared with solar wind data obtained from the ACE satellite in low-earth orbit to verify the model. Since it takes a few days for the solar wind to reach the earth's orbit from the solar surface, it seems theoretically possible to predict space weather a few days in advance with a degree of practical precision by enhancing the precision of the simulator for the sun and the solar wind, and integrating it with a model of the magnetosphere, ionosphere and atmosphere.

References

- 1 Schunk, R. W. and J. C. G. Walker, "Theoretical ion densities in the lower ionosphere," *Planet. Space Sci.*, Vol. 21, pp. 1875–1896, 1973.
- 2 Sojka, J. J. and R. W. Schunk, "A theoretical study of the global F-region for June solstice, solar maximum, and low magnetic activity," *J. Geophys. Res.*, Vol. 90, pp. 5285–5298, 1985.
- 3 Fuller-Rowell, T. J. et al., "Interactions between neutral thermospheric composition and the polar ionosphere using a coupled ionosphere-thermosphere model," *J. Geophys. Res.*, Vol. 92, pp. 7744–7748, 1987.
- 4 Roble., R. G., E. C. Ridley, A. D. Richmond, and R. E. Dickinson, "A coupled thermosphere/ionosphere general circulation model," *Geophys. Res. Lett.*, Vol. 15, No. 12, pp. 325–328, 1988.
- 5 Roble., R. G. and E. C. Ridley, "A thermosphere-ionosphere-mesosphere-electrodynamics general circulation model (TIME-GCM): Equinox solar cycle minimum simulations (30–500 km)," *Geophys. Res. Lett.*, Vol. 21, No. 6, pp. 417–420, 1994.
- 6 Raeder, J., Y. L. Wang, and T. J. Fuller-Rowell, "Geomagnetic storm simulation with a coupled magnetosphere-ionosphere-thermosphere model," in *Space Weather: Progress and Challenges in Research and Applications*, pp. 377–384, P. Song, H.J. Singer, and G. Siscoe, editors, Geophysical Monograph, No. 125, AGU, Washington, D.C., 2001.
- 7 Tóth, G., D. L. De Zeeuw, T. I. Gombosi, W. B. Manchester, A. J. Ridley, Igor V. Sokolov, and I. I. Roussev, "Sun-to-thermosphere simulation of the 28–30 October 2003 storm with the Space Weather Modeling Framework," *Space Weather*, Vol. 5, S06003, doi: 10.1029/2006SW000272, 2007.

-
- 8 Jin, H., Y. Miyoshi, H. Fujiwara, and H. Shinagawa, "Electrodynamics of the formation of ionospheric wave number 4 longitudinal structure," *J. Geophys. Res.*, Vol. 113, No. A09307, doi: 10.1029/2008JA013301, 2008.
 - 9 Richards, P. G., J. A. Fennelly, and D. G. Torr, "EUVAC: A Solar EUV Flux Model for Aeronomic Calculations," *J. Geophys. Res.*, Vol. 99, No. A5, pp. 8981–8992, 1994.
 - 10 Hedin, A. E., "Extension of the MSIS thermosphere model into the middle and lower atmosphere," *J. Geophys. Res.*, Vol. 96, pp. 1159–1172, 1991.
 - 11 Fuller-Rowell, T. J. and D. Rees, "Derivation of a conservation equation for mean molecular weight for a two constituent gas within a three-dimensional, time-dependent, model of the thermosphere," *Planet. Space Sci.*, 31, 1209–1222, 1983.
 - 12 Hedin, A. E., E. L. Fleming, A. H. Manson, F. J. Schmidlin, S. K. Avery, R. R. Clark, S. J. Franke, G. J. Fraser, T. Tsuda, F. Vial, and R. A. Vincent, "Empirical wind model for the upper, middle and lower atmosphere," *J. Atmos. Terr. Phys.*, Vol. 58, pp. 1421–1447, 1996.
 - 13 Miyoshi, Y. and H. Fujiwara, "Day-to-day variations of migrating diurnal tide simulated by a GCM from the ground surface to the exobase," *Geophys. Res. Lett.*, Vol. 30, No. 5, pp. 1789–1792, doi: 10.1029/2003GL017695, 2003.
 - 14 Liu, H., H. Lühr, V. Henize, and W. Köhler, "Global distribution of the thermospheric total mass density derived from CHAMP," *J. Geophys. Res.*, Vol. 110, No. A04301, doi: 10.1029/2004JA010741, 2005.
 - 15 Liu, H., S. Watanabe, and T. Kondo, "Fast thermospheric wind jet at the Earth's dip equator," *Geophys. Res. Lett.*, Vol. 36, No. L08103, doi: 10.1029/2009GL037377, 2009.



SHINAGAWA Hiroyuki, Ph.D.

*Senior Researcher, Space Environment
Group, Applied Electromagnetic
Research Center
Ionospheric Physics*